Chapter 4

Phase structure of lattice QCD

Understanding the phase structure of lattice QCD is an important pre-requisite before starting large scale simulations [113]. As we will see below, the main result of this chapter is that Wilson type fermions generically show a first order phase transition around the chiral point for lattice spacings below a certain threshold. The existence of this first order phase transition, which is due to lattice artifacts, has important consequences for simulations with this kind of lattice fermions.

First, approaching the "physical point", at which the pion mass assumes its value as measured in experiment, the algorithms used in lattice simulations suffer from a substantial slowing down, as explained in the previous chapter. Since simulations are also restricted to finite lattice spacings, lattice QCD in general involves extrapolations to the physical point and to the continuum. In order to be able to control those extrapolations it is necessary to know whether there is indeed a smooth extrapolation possible.

Second, numerical simulations in the vicinity of first or second order phase transitions are problematic. It is not obvious whether the algorithms correctly sample configuration space in such a situation. And, assuming they do so, usually one observes practical problems such as long thermalization and autocorrelation times. Therefore, as – unlike the finite temperature case – the phase transition itself is not the topic under investigation, one would like to avoid to simulate close to a phase transition.

It is important to realize that the above mentioned first order phase transition for Wilson type lattice fermions imposes a lower bound on the value of the pseudo scalar mass that can be simulated at a given lattice spacing. The actual value of the lower bound to the pseudo scalar mass, however, turns out to depend on the particular gauge action discretization providing an opportunity to circumvent or at least reduce the aforementioned complications.

We remark that strictly speaking in a finite volume with a finite number of lattice

points there cannot exist a phase transition. Nevertheless, already in a finite, but large enough volume the effects of a phase transition in infinite volume can be visible and rather strong.

For QCD it is widely believed that chiral symmetry is spontaneously broken by the ground state and one expects a first order phase transition where the scalar condensate jumps from negative to positive value when the mass is changed from small negative to small positive values, or vice versa. In this chapter we are going to discuss in lattice chiral perturbation theory how the explicit chiral symmetry violations of Wilson type fermions at non-vanishing lattice spacing will affect the continuum picture, which will allow an interpretation of our numerical results. Thereafter, we will present our numerical results on the phase structure of lattice QCD in a regime of lattice spacings where so far a systematic study was missing. These results will provide evidence for a first order phase transition, as mentioned before. Finally, we will outline how to reduce the effects of this phase transition by choosing a different discretization of the gauge part in the action.

4.1 Effective potential model

As we have discussed in section 1.2.2, the massless Lagrangian of QCD for two flavors of quarks is symmetric under the chiral group $\mathrm{SU}_V(2) \times \mathrm{SU}_A(2)$, which is spontaneously broken down to $\mathrm{SU}_V(2)$ by the ground state of the theory. To describe reality the Lagrangian contains a quark mass term explicitly breaking the aforementioned symmetry. Therefore the vector and axial currents are not exactly conserved.

However, since the masses of up- and down-quark are small, also the divergence of the currents vanishes approximately and the masses might be treated as a small perturbation to the massless theory as is done in the chiral perturbation theory (χPT) [135, 136, 137]. From a principle point of view lattice calculations include all the low energy structure of QCD with the quark masses being free parameters. Therefore, there is a priori no need for a χPT if expectation values can be computed on the lattice on a non-perturbative level at realistic values of the quark mass. However, nowadays lattice calculations are not yet able to provide reliable results obtained with values of the quark masses as small as estimated in experiment.

Hence, χPT might serve as an useful tool to connect the results for physical quantities obtained from lattice simulations performed at un-physically large quark masses with those at the physical point. However, χPT is valid only for small quark masses below a certain upper bound or in different words it has a finite convergence radius, which allows to make contact to lattice calculations if and only if lattice simulations with masses below this bound are possible. The actual value of this

bound is unknown, but lattice simulations with pion masses below 300 MeV will most likely be needed.

As originally χPT is an effective low energy theory of continuum QCD, it is not valid at finite values of the lattice spacing a. However, one can also formulate an effective theory including the lattice spacing, which is then treated as a small, additional parameter.

4.1.1 Chiral perturbation theory on the lattice

In section 1.2.3 we have introduced the Symanzik effective theory, which is expected to describe the lattice theory close to the continuum by an effective continuum Lagrangian. The usual terms in the continuum Lagrangian are supplemented by contributions proportional to powers of the lattice spacing. We have also discussed in section 1.2.3 that the effective fermionic Lagrangian is of the form (see Eq. (1-44))

$$\mathcal{L}_{\text{eff}} \sim \bar{\psi}(\gamma_\mu D_\mu + m)\psi + c_{\text{sw}} a \bar{\psi} i \sigma_{\mu\nu} F_{\mu\nu} \psi + \mathcal{O}(a^2)\,. \tag{4-1}$$

This amounts to QCD with a Pauli term. And since the Pauli term transforms under chiral rotations exactly like a mass term [41], the corresponding chiral Lagrangian is already known.

We will not discuss lattice χPT (LχPT) in detail, as it can for instance be found for Wilson lattice QCD in [138], but we rather follow the qualitative discussion of reference [41] to immediately access the phase structure of lattice QCD at small quark masses.

In terms of a SU(2) matrix-valued field Σ, transforming under independent SU(2) rotation U_L and U_R as $\Sigma \to U_L \Sigma U_R^\dagger$ the kinetic part (which is the chiral Lagrangian in absence of mass and Pauli term) can be written as

$$\mathcal{L}_\chi = \frac{f_\pi^2}{4} \operatorname{Tr}\Big(\partial^\mu \Sigma^\dagger \partial_\mu \Sigma\Big)\,, \tag{4-2}$$

and the potential energy is given by

$$\mathcal{V}_\chi = -\frac{c_1}{4} \operatorname{Tr}\Big(\Sigma + \Sigma^\dagger\Big) + \frac{c_2}{16} \Big\{\operatorname{Tr}\Big(\Sigma + \Sigma^\dagger\Big)\Big\}^2 \tag{4-3}$$

with coefficients $c_1 \sim m\Lambda_{\text{QCD}}^3 + a\Lambda_{\text{QCD}}^5$ and $c_2 \sim m^2\Lambda_{\text{QCD}}^2 + ma\Lambda_{\text{QCD}}^4 + a^2\Lambda_{\text{QCD}}^6$. The factors or Λ_{QCD} are required by dimensional analysis and dimensionless coefficients of order unity are dropped [41]. In the following we will be particularly interested in the case where $m' = m - a\Lambda_{\text{QCD}}^2 \sim a^2\Lambda_{\text{QCD}}^3$. In this regime the coefficients can be simplified to

$$c_1 \sim m'\Lambda_{\text{QCD}}^3\,, \qquad c_2 \sim a^2\Lambda_{\text{QCD}}^6\,. \tag{4-4}$$

In this situation the two terms in the potential energy become comparable, since $c_1 \sim c_2$, and it will lead to the prediction of a non-trivial phase structure of Wilson lattice QCD for small quark masses. Moreover, the coefficient c_1 parameterizes the bare quark mass and c_2 is proportional to a^2.

By denoting with A the flavor singlet component of Σ, the latter can be expressed like

$$\Sigma = A + i \sum_{r=1}^{3} B_r \tau_r \,, \tag{4-5}$$

with $1 = A^2 + \sum B_r B_r$ and τ_r the three Pauli matrices. This constrains A, which corresponds to the scalar condensate, to lie between -1 and 1 inclusive. The potential then reads

$$\mathcal{V}_\chi = -c_1 A + c_2 A^2 = A(c_2 A - c_1) \,. \tag{4-6}$$

Note that B_3 corresponds to $\langle \bar{\psi} \gamma_5 \tau_3 \psi \rangle$.

In order to find the ground state Σ_0 the effective potential has to be minimized. Σ can then be expanded around Σ_0 and observables like pion masses can be extracted in terms of the quark mass, c_2 and the pion decay constant f_π. And it turns out that the results depend strongly on the sign of the coefficient c_2, which parameterizes the lattice artifacts.

In case of *positive* c_2 there exists a phase in the region of bare quark masses defined by $-2c_2 < c_1 < 2c_2$ where the flavor symmetry is broken. This expresses itself in massless charged pions, because they are Goldstone bosons of spontaneous flavor symmetry breaking, but a massive uncharged pion.

At the boundaries $c_1 = \pm 2c_2$ all three pions are massless and the system undergoes a second order phase transition, while outside the phase with ($|c_1| > 2c_2$) the flavor symmetry is preserved by the ground state and all three pions are massive. This scenario is called the *Aoki scenario*, because S. Aoki first predicted the existence of such a flavor symmetry breaking phase [139, 140, 141].

The alternative is that c_2 is *negative*. In this case the flavor symmetry is preserved in the whole range of values for c_1, but it does not exist a value of c_1 where the pions are massless, since the pion masses are given by [41]

$$m_\pi^2 = \frac{1}{f_\pi^2}(|c_1| + 2|c_2|) \,. \tag{4-7}$$

At $c_1 = 0$ the vacuum expectation value of Σ jumps from $A = -1$ to $A = +1$. Since this jump appears at non-zero pion mass the thermo-dynamical description of the behavior near $c_1 = 0$ corresponds to a first order phase transition.

This situation is called *normal scenario* due to its similarity to the continuum first order chiral phase transition around zero quark mass. In the continuum, of course, the pions as Goldstone bosons become massless in the chiral point in contrast

to a non-zero minimal value of the pion mass characterizing the normal scenario on the lattice.

The minimal value of the squared pion mass is in LχPT for vanishing value of c_1 proportional to c_2, which is of $\mathcal{O}(a^2)$. This means, if a negative value of c_2 is realized in Wilson lattice QCD the minimal value of m_π^2 will vanish like a^2 when the continuum limit is performed. On the other hand, if the Aoki scenario is realized, the width of the Aoki phase will vanish like $\Delta m \sim a^3$ [41]. Unfortunately LχPT by itself is not able to make any prediction about the sign of c_2.

Although the just discussed phase structure for Wilson lattice QCD from LχPT is known already quite some time [41], the corresponding investigation for the Wilson twisted mass formulation of lattice QCD was missing. It was published in Refs. [142, 97, 143] only after we published parts of the results that will be presented in this chapter. The introduction of a twisted mass term in the low energy effective Lagrangian turns out to be straightforward. The only difference is one additional term in the effective potential energy

$$\mathcal{V}_\chi = -c_1 A - c_3 B_3 + c_2 A^2 \,. \tag{4-8}$$

The new coefficient $c_3 \sim \mu$ is parameterizing the twisted mass in the effective theory while the other coefficients are given as in the former discussion. If we now consider values of $m' \sim \mu \sim a^2\Lambda_{\mathrm{QCD}}^3$ we again have to distinguish between negative and positive values of c_2. The sign of c_3 depends on the value of μ, which we choose to be positive, since it does not influence the qualitative picture of the phase structure.

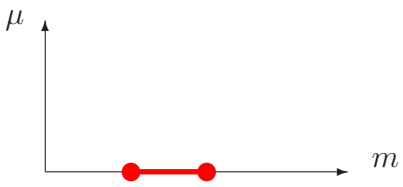

Figure 4.1: Phase diagram in the $m - \mu$ plane for the Aoki scenario.

For $c_2 > 0$ and $\mu \neq 0$ fixed the Aoki scenario changes as follows: charged and uncharged pions are massive for all values of c_1, even though the flavor SU(2) symmetry is explicitly broken. The value A changes continuously as a function of c_1 and there is no phase transition. The situation for $c_2 > 0$ is summarized schematically in figure 4.1. For $\mu = 0$ the two second order phase transition points are indicated by the filled circles. On the line between these two circles the charged pions are massless and the uncharged pion is massive. Note that this line corresponds to a first order transition line where B_3 jumps when the values of μ sweep across zero.

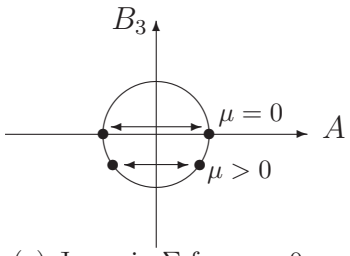

(a) Jump in Σ for $c_1 = 0$.

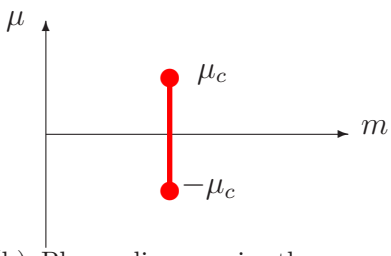

(b) Phase diagram in the $\mu - m$ plane.

Figure 4.2: Phase diagram and jump in Σ for the normal scenario ($c_2 < 0$).

In the case of $c_2 < 0$ the influence of a non-zero value for the twisted mass parameter μ is different. Here μ plays the rôle of a "magnetic field" and shifts away the minimum of the potential $\mathcal{V}_\chi$ from the values $A = \pm 1$. As indicated in figure 4.2(a) B_3 adopts a non-zero value and $|A| < 1$. With increasing modulus of μ the two minima of the potential approach each other and the transition line has an endpoint for

$$\mu_c \sim a^2 \,. \tag{4-9}$$

For $\mu \neq 0$ flavor and parity symmetry are explicitly broken and at $\mu = \mu_c$ the uncharged pion becomes massless while the charged pions remain massive. At $c_1 = 0$ and $\mu < \mu_c$ a first order phase transition takes place. The corresponding phase diagram is schematically represented in figure 4.2(b), where we indicate the endpoints of the first order transition line at μ_c by filled circles.

Before turning to a numerical check of LχPT it is useful to summarize what was known in the literature so far about the phase structure of Wilson lattice QCD. In a recent re-investigation [144, 145] of the Aoki phase with the Wilson gauge action for values of the coupling $\beta < 5$ the authors found in agreement with previous publications [146, 141, 147, 148, 149] evidence for an Aoki phase only for values of $\beta < 4.6$. On the other hand, for values of $\beta = 4.6$ and $\beta = 5$ they found no evidence for the realization of an Aoki scenario.

For values of $\beta > 5$ (Wilson plaquette gauge action), however, a systematic investigation of the phase structure was missing. Even though there exist several indications in the literature (see for instance [150]) for the realization of the normal scenario in this region of β values the connection to the aforementioned results from LχPT was never explicitly mentioned.

4.2 Numerical results

4.2.1 Simulation points

We have chosen three values of the bare coupling constant β to study the phase structure of lattice QCD with Wilson plaquette gauge action and Wilson twisted mass fermions. The simulation parameters can be found in table 4.1. The values of $a\mu$ were chosen such that $r_0\mu$ is roughly constant for all values of β. Moreover, the lattice sizes were taken to have a physical volume of at least 2 fm in order to allow for save extraction of meson physics.

The values of the lattice spacing quoted in table 4.1 are estimates to give an orientation. At $\beta = 5.2$ we have in addition to the lattice size quoted in table 4.1 results for $16^3 \times 32$ lattices to check for finite volume effects.

β	$L^3 \times T$	$a\mu$	a [fm]
5.1	$12^3 \times 24$	0.013	0.20
5.2	$12^3 \times 24$	0.010	0.16
5.3	$16^3 \times 32$	0.008	0.14

Table 4.1: Simulation points for Wilson plaquette gauge action.

For the next subsections we will mainly concentrate on the results obtained at $\beta = 5.2$, because the results are qualitatively the same for the three values of β. After this description of the first order phase transition phenomenon we will in a next step analyze also the scaling with the lattice spacing. For all these investigations we used the hopping parameter representation of the Wilson twisted mass lattice action in the twisted basis as given by Eq. (1-46).

4.2.2 Thermal cycles

We started our investigation of the phase diagram of zero temperature lattice QCD by performing thermal cycles in κ while keeping fixed $\beta = 5.2$ and the value of the twisted mass parameter $a\mu$. These cycles are performed such that a starting value of κ_{start} is chosen and then κ is incremented, without performing further intermediate thermalization sweeps, until a final value of κ_{final} is reached. At this point the procedure is reversed and κ is decremented until the starting value κ_{start} is obtained back. At each value of κ 150 configurations are produced and averaged over.

In fig. 4.3 we show three such thermal cycles, performed at $a\mu = 0$, $a\mu = 0.01$ and $a\mu = 0.1$ from bottom to top. In the cycles signs of hysteresis effects can be seen for $a\mu = 0$ and $a\mu = 0.01$ while for the largest value of $a\mu = 0.1$ such

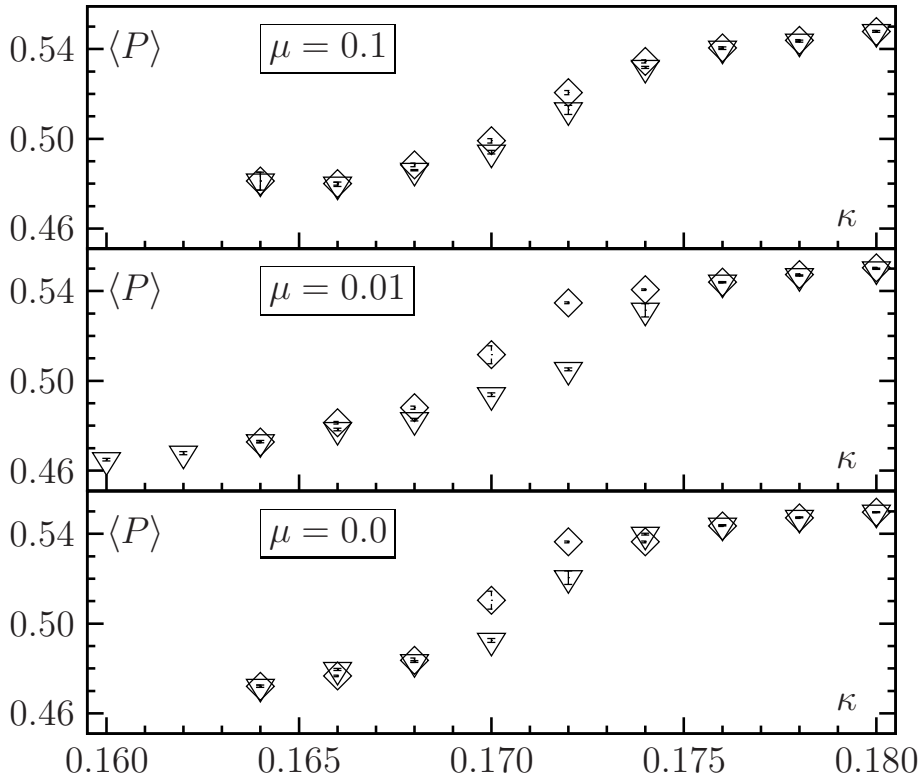

Figure 4.3: Thermal cycles in κ on $8^3 \times 16$ lattices at $\beta = 5.2$. The plaquette expectation value is shown for $a\mu = 0.1$, $a\mu = 0.01$ and $a\mu = 0$ (top to bottom). The triangles refer to increasing κ-values, the diamonds to decreasing ones. The errors are the naive statistical errors, without taking the autocorrelation time into account.

effects are hardly visible. Hysteresis effects in thermal cycles *may be* signs of the existence of a first order phase transition. However, they should only be taken as first indications. Nevertheless, they provide most useful hints for further studies to search for meta-stable states.

4.2.3 Meta-stabilities

Guided by the results from the thermal cycles, we next performed simulations at fixed values of $a\mu$ and κ, starting with ordered and disordered configurations, staying again at $\beta = 5.2$. In fig. 4.4 we show the Monte Carlo time evolution of the plaquette expectation value, in most cases on a $12^3 \times 24$ lattice. For several values of κ we find coexisting branches with different average values of the plaquette. The gap (the "latent heat") appears to be rather large. At $\kappa = 0.1717$ we show the history of the plaquette expectation value also on a larger $(16^3 \times 32)$ lattice. It seems that the gap in the plaquette expectation value does not depend much on the lattice size, suggesting that the meta-stability we observe here is not a finite volume effect. In most cases the twisted mass is $a\mu = 0.01$, except for the picture right in the upper

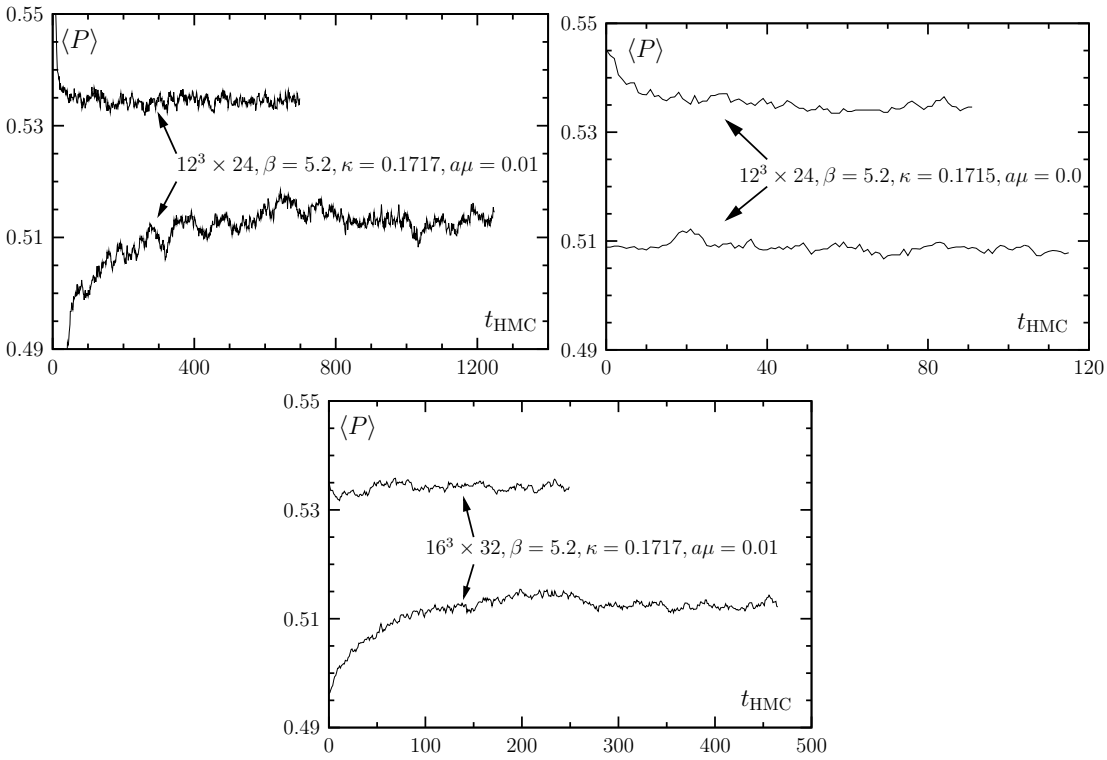

Figure 4.4: Meta-stable states at $\beta = 5.2$. The plaquette value is plotted as a function of the HMC time, i.e. the number of trajectories. The lattice size is $12^3 \times 24$ except for the bottom figure where it is $16^3 \times 32$. The value for the twisted mass parameter is $a\mu = 0.01$ except for the rightmost figure where it is $a\mu = 0$.

line where it is $a\mu = 0$. Since the meta-stabilities are also observed with $a\mu = 0$ it is already excluded that the phenomenon is only due to the twisted mass term.

The lifetime of a meta-stable state, i.e. the time before a tunneling to the stable branch occurs, depends on the algorithm used. In fact, one may wonder, whether the appearance of the meta-stable states seen in fig. 4.4 may not be purely an artefact of our algorithms. We cannot completely exclude this possibility but we believe it is very unlikely: we employed two very different kinds of algorithms in our simulations as explained in subsection 1.4.2. We observe the meta-stable states with both, the HMC and the TSMB algorithm. We also inter-changed configurations between the two algorithms: a configuration generated with algorithm A was iterated further with algorithm B and vice versa. We find that in such situations the plaquette expectation value remains in the state where it has been before the interchange of configurations took place. In addition, as we shall see below, the two states can be characterized by well defined and markedly different values of basic physical quantities. We therefore conclude that the meta-stable states are a generic phenomenon of lattice QCD in the Wilson or Wilson twisted mass formulation. This conclusion is strongly supported by the fact that it is consistent with the picture provided by

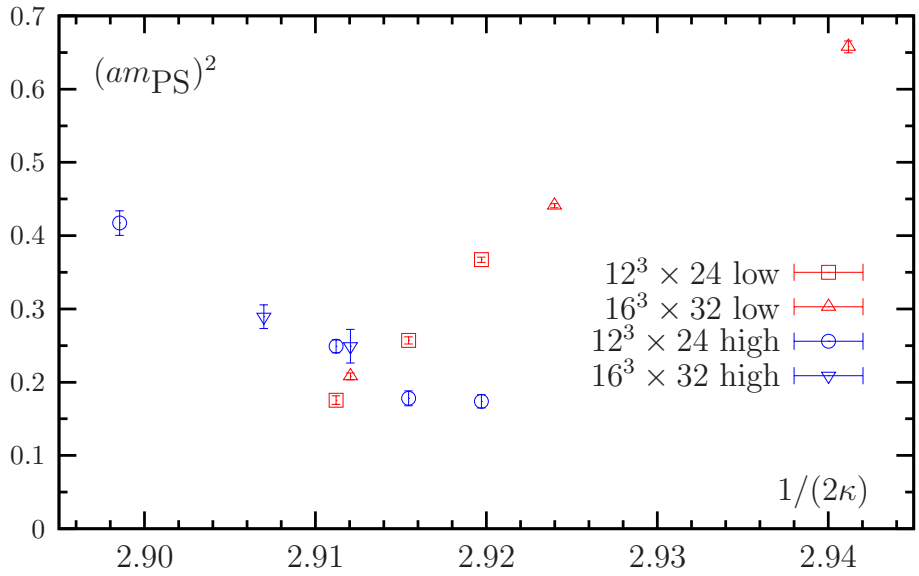

Figure 4.5: The pseudo scalar mass squared in lattice units as a function of $1/(2\kappa)$ on two lattice sizes measured separately on configurations in the two (meta)stable states. These runs were performed at $\beta = 5.2$ and $a\mu = 0.01$.

LχPT, which we discussed in section 4.1.1.

4.2.4 Pseudo scalar and quark masses

While in the preceding paragraph we looked at the plaquette expectation value indicating a first order phase transition we will discuss this phenomenon in the following paragraph in terms of pseudo scalar and quark masses. To this end we selected separately configurations with high and with low plaquette expectation value and measured the pseudo scalar mass $m_{\rm PS}$ and the untwisted PCAC quark mass $m_\chi^{\rm PCAC}$, which we obtained as explained in section 1.3.

In fig. 4.5 we show the pseudo scalar mass squared in lattice units as a function of $1/(2\kappa)$. We observe that the pseudo scalar mass is rather large and the most striking effect in the graph is that it can have two different values at the same κ value. Moreover, the minimal value of the pseudo scalar mass is not zero, but assumes a rather large value.

If we consider the quark mass $m_\chi^{\rm PCAC}$ in fig. 4.6, we see that in the states with a low plaquette expectation value the mass is positive while for high values of the plaquette expectation it is negative. These quark masses with opposite sign coexist for some values of κ.

Figs. 4.4-4.6 clearly reveal that for small enough values of μ meta-stabilities show up in the quantities we have investigated, such as $m_{\rm PS}$, $m_\chi^{\rm PCAC}$ and the average plaquette, if m_0 is close to its critical value. What "small enough μ" means is

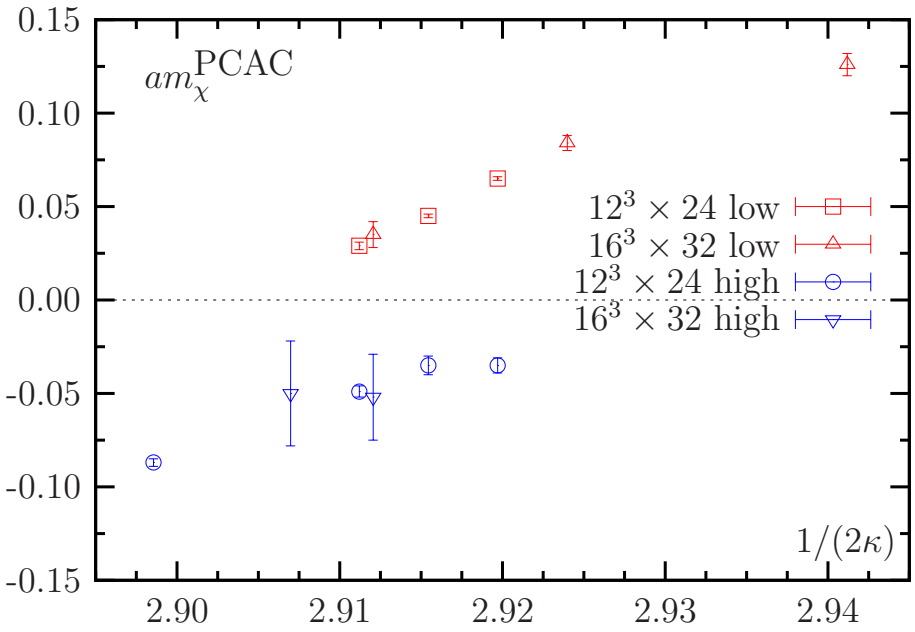

Figure 4.6: The PCAC quark mass $m_\chi^{\rm PCAC}$ in lattice units as defined in Eq. (1-80) as a function of $1/(2\kappa)$ on two lattice sizes measured separately on configurations in the two (meta)stable states. The values of $\beta = 5.2$ and $a\mu = 0.01$ are fixed.

likely to change with β, see below. As a matter of fact, when m_0 is significantly larger (smaller) than $m_{\rm crit}$ we find $m_\chi^{\rm PCAC}$ to be positive (negative) and no signal of meta-stabilities.

Of course, one might ask the question how we can know that the values of m_0 are close to its critical value, since we do not observe any value for m_0 where $m_\chi^{\rm PCAC} = 0$. The answer to this question is that – as argued already above – in a finite volume there exist no phase transition and therefore, $m_\chi^{\rm PCAC}$ must be an analytical function of m_0. Only due to the disability of the algorithm to correctly sample configuration space in this region of m_0 values, we get the impression (on the remnant) of a first order phase transition. Analyticity in turn implies that in the region of meta-stabilities an optimal algorithm would find a value of m_0 where $m_\chi^{\rm PCAC} = 0$, which is, however, a finite volume effect: in infinite volume physical observables such as $m_\chi^{\rm PCAC}$ jump at the phase transition point and hence, $m_\chi^{\rm PCAC}$ does not become zero. The chiral point is then defined at the phase transition point.

The remark that meta-stabilities take place for m_0 close to its critical value is important for the interpretation of the observed phenomenon. As we explained in section 4.1, LχPT predicts two different scenarios for the phase structure at small quark masses. The so called normal scenario is characterized as follows: firstly, a first order phase transition appears when the untwisted quark mass sweeps across zero as long as the twisted mass parameter is smaller than a critical value μ_c. Secondly, the pseudo scalar mass has a minimal value that is larger than zero.

As meta-stabilities are expected to take place in the vicinity of a first order phase transition, we therefore conclude that at this value of β the normal scenario is realized.

Even though we discussed in this subsection only one value of β, the same phenomenon appears for $\beta = 5.1$ and for $\beta = 5.3$: we observe meta-stabilities and a non-zero value of the minimal pseudo scalar mass. In order to simplify the language, we denote simulation points in the phase with high plaquette expectation value with "high", and correspondingly the simulation points with low plaquette expectation value with "low".

The dependence of the phase transition on the lattice spacing will be the topic of the following subsection.

4.2.5 The phase transition as a function of the lattice spacing

As mentioned already before, we have apart from $\beta = 5.2$ also simulation points with $\beta = 5.1$ and $\beta = 5.3$. The details for all our simulation points can be found in tables 4, 5, and 6 of Ref. [151]. The values of $a\mu$ were fixed for each β value such that $r_0\mu \approx 0.03$ for all values of β. Note that the value of r_0/a depends on the value of the quark mass and therefore, we had to choose a reference value for r_0/a. We have chosen this reference point to have $(r_0 m_{\mathrm{PS}})^2 = 1.5$ and interpolated our data for $\beta = 5.1$ and $\beta = 5.3$ to this point, while for $\beta = 5.2$ a short extrapolation was necessary. We again used the ROOT and MINUIT packages from CERN to perform the corresponding fits. The parameters are summarized in table 4.1.

In figure 4.7 we have plotted the plaquette expectation value $\langle P \rangle$ as a function of $1/(2\kappa)$ for the three values of β. The β-dependence shows that the gap in the plaquette expectation value ΔP decreases substantially when moving from $\beta = 5.1$ ($a \approx 0.20$ fm) to $\beta = 5.3$ ($a \approx 0.14$ fm). One possible definition for the quantity ΔP is the difference between low and high phase plaquette expectation value at the smallest value of κ where a meta-stability occurs. Moreover, one can see in figure 4.7 that the meta-stability region in $1/(2\kappa)$ gets narrower with increasing values of β. Other quantities than ΔP show a similar behavior. Also the gap in m_χ^{PCAC} between positive and negative values shrinks significantly with increasing values of β.

We remark that the first order phase transition exists also in the continuum limit where it occurs as the jump of the scalar condensate as a consequence of spontaneous chiral symmetry breaking. Of course, in the continuum limit, the phase transition occurs only for $\mu = 0$ and the jump in $\langle P \rangle$ will disappear.

An interesting practical question is, at what value of the lattice spacing a the minimal pseudo scalar mass $m_{\mathrm{PS}}^{\mathrm{min}}$ that can be simulated without meta-stability as-

β	r_0/a	$r_0\mu$	ΔP	$m_{\rm PS}^{\rm min}$[MeV]
5.1	2.497(29)	0.0327	0.0399(1)	$\gtrsim 600$
5.2	3.124(85)	0.0312	0.0261(1)	$\gtrsim 630$
5.3	3.628(60)	0.0290	0.0077(4)	$\gtrsim 470$

Table 4.2: Reference values for r_0/a together with $r_0\mu$, the plaquette gap ΔP and $m_{\rm PS}^{\rm min}$ for the three β values.

sumes a value of, say, 300 MeV. At such a value contact to χPT could be established. Unfortunately, the precise determination of the meta-stability region in κ and of a minimal pseudo scalar mass is very difficult. We can estimate the meta-stability region in κ from our data by including all κ values where meta-stabilities occur. A lower bound for the minimal pseudo scalar mass in the low plaquette phase (high plaquette phase) is then represented by the value of $m_{\rm PS}$ at the lower (higher) end of this κ interval. In the following we will mainly focus on the low plaquette phase since this is the natural choice for studying lattice QCD.

We give in table 4.2 estimates for the minimal pseudo scalar masses in the low plaquette phase in physical units. In addition, we provide estimates for ΔP. In principle, it would be the natural next step to extrapolate the minimal pseudo scalar mass and ΔP as a function of the lattice spacing. However, our present data do not allow for a reliable and safe extrapolation. First of all, the determination of the minimal pseudo scalar mass has a large ambiguity in itself since we do not know for sure, which simulation point is stable or meta-stable. Second, the only three values of β we have used give a too short lever arm to perform a trustworthy extrapolation. And, last, the values of r_0/a are very different in the two phases, which makes it particularly difficult to follow ΔP as a function of the lattice spacing, since ΔP contains information from both phases.

Nevertheless, an estimate on a more qualitative level yields a value of the lattice spacing of $a \sim 0.07$ fm $- 0.1$ fm where simulations with pseudo scalar masses of about 300 MeV can be performed without being affected by the first order phase transition*.

At this point we can complete the picture of the phase structure of lattice QCD with Wilson type quarks. It is schematically plotted in figure 4.8 in the β-μ-κ-space on the basis of the predictions of LχPT and the numerical findings as presented in this section and in the literature. For values of β smaller than about five it was found that the Aoki scenario is realized [144, 145]. The phase is located around the critical value of κ, its width in κ diminishes with increasing values of β and, as

*We remark that we have indications for meta-stabilities even at the parameters of run D from the last chapter, i.e. $a \sim 0.08$ fm, $\mu = 0$ and $m_{\rm PS} \sim 300$ MeV. However, this might turn out to be a thermalization phenomenon.

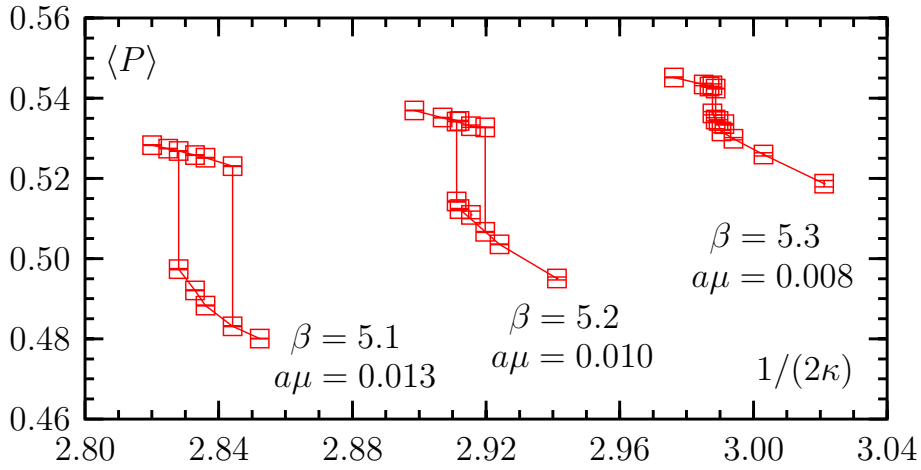

Figure 4.7: Evolution of the gap in the plaquette expectation value for the three values of β.

discussed in section 4.1, the Aoki phase disappears for non-vanishing values of μ. The resulting area is plotted in dark-gray in figure 4.8. On the boundaries of this area a second order phase transition takes place.

Since the first order phase transition in the normal scenario takes place for κ equal to its critical value and values of $|\mu|$ smaller than the critical value μ_c, the corresponding area of first order phase transition points is orthogonal to the Aoki phase area. It is plotted in light-gray in figure 4.8. As discussed in section 4.1 the value of μ_c goes to zero as a^2 when the continuum limit is approached. Therefore the width of the first order phase transition area gets correspondingly smaller. On the boundary of this area are second order endpoints located.

In the region of β values between the two scenarios there are no data available describing how the crossover exactly looks like. The design of this crossover as it is plotted in figure 4.8 is a guess under the assumption that the two scenarios do not exist in parallel for the same set of parameters and that the crossover is smooth in β. However, this brings the discussion to the question how reliable predictions of LχPT are, when the lattice spacing is larger than 0.15 fm. If LχPT to order a^2 would explain the phase structure for the whole above mentioned range of lattice spacings, the sign of c_2 must change as a function of β.

We cannot answer this question, even though we think that it is very likely that higher order lattice artefacts contribute significantly to the phase structure if the lattice spacing is large. These higher order effects could then also avoid the necessity of a sign change in c_2, because the crossover can then be explained by higher order lattice artifacts.

Finally, let us discuss the implications of the observed phase structure on simulations in lattice QCD with Wilson like fermions. First of all the understanding of

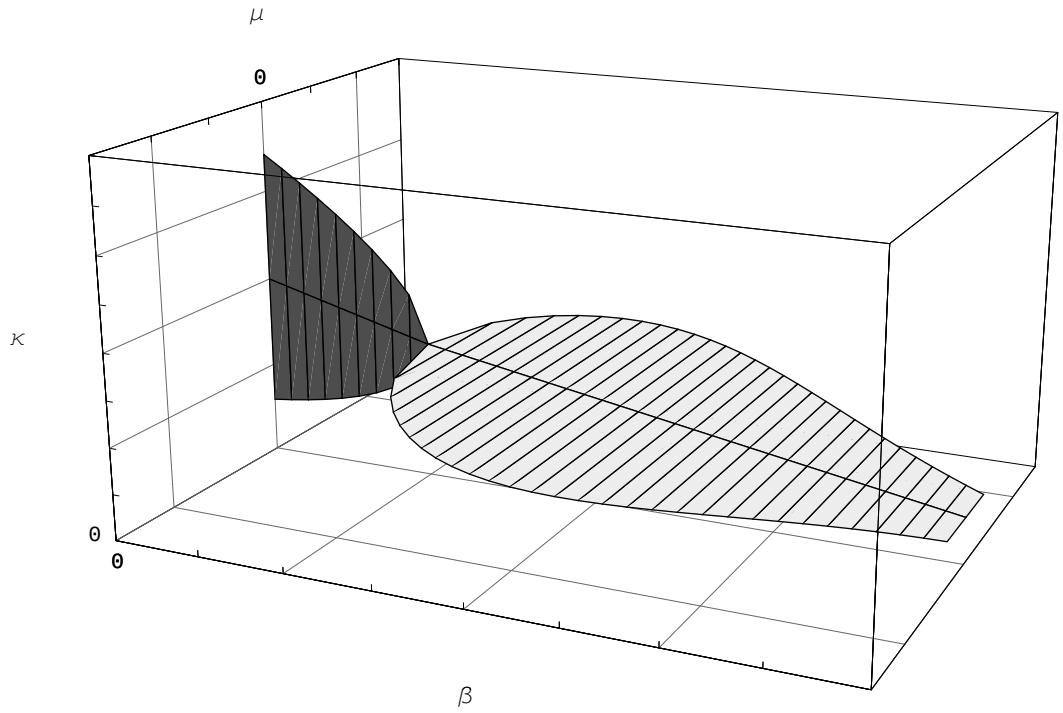

Figure 4.8: Schematic phase-diagram of Wilson twisted mass lattice QCD. The light-gray surface is the area where a first order phase transition takes place ($c_2 < 0$) when κ is crossing its critical value. At the boundary of this area a second order endpoint is located. The dark-gray area is the parameter region where the Aoki scenario is realized ($c_2 > 0$). At the border line of this area a second order phase transition takes place. At the value of β where the two areas touch each other, c_2 is supposed to be identically zero.

the phase structure is (or should be) an important pre-requisite for any large scale simulation in lattice QCD, a piece of information that was missing so far.

Unfortunately, from an only practical point of view the actual phase structure makes simulations with Wilson gauge action and Wilson like fermions difficult, if not unfeasible. The reason is the following: due to the meta-stability phenomenon simulations with pseudo scalar masses of the order of 300 MeV must be performed with lattice spacings of $a \lesssim 0.1$ fm and correspondingly large volumes in lattice units. To perform then a reliable continuum extrapolation simulations with at least two even smaller lattice spacings with the same physical volumes are needed. All together large scale simulations in this setup become rather demanding, and are therefore not realistic.

Note that in the two dimensional Gross-Neveu model [152] it is possible to compute the phase structure analytically. Depending on the parameters the outcome is very similar to the phase structure as observed for Wilson lattice QCD [153, 154, 155, 156].

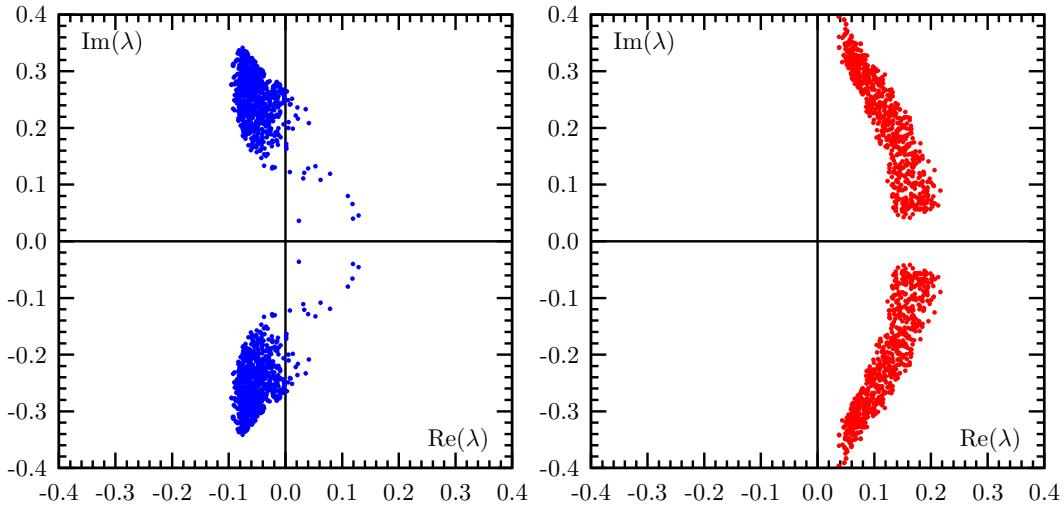

(a) High plaquette phase. (b) Low plaquette phase.

Figure 4.9: Eigenvalues λ of the Wilson twisted mass fermion matrix with small absolute value in case of the Wilson plaquette action at $\beta = 5.2$, $\mu = 0.01$, $\kappa = 0.1715$ on a $12^3 \times 24$ lattice. Both high plaquette and low plaquette spectra are shown.

4.2.6 Changing the gauge action

As explained above we think that simulations with Wilson plaquette gauge action and Wilson like fermions are not feasible due to the existence of the first order phase transition. This is of course a rather un-satisfactory result and a cure is needed if one wants to stick to Wilson twisted mass fermions in order to use the automatic $\mathcal{O}(a)$ improvement property of mtmQCD.

If one compares the infra-red end of the eigenvalue spectrum of the twisted mass operator at identical parameters, but on gauge configurations from the high and the low plaquette phase separately as we show it in figure 4.9[†], one can see that the first order phase transition is visible as a strong difference in infra-red spectrum. Therefore, the phase structure might be influenced by changing the infra-red eigenvalue spectrum, which is well known to be possible by changing the discretization of the gauge action (see for instance [157, 158, 159, 160]). In fact, the JLQCD collaboration reported in Refs. [150, 161] for lattice QCD $N_f = 3$ non perturbatively improved flavors of quarks that the meta-stability phenomenon disappears when the Iwasaki gauge action [162, 163] or the tadpole improved Symanzik gauge action [13] is used instead of the Wilson plaquette gauge action.

In order to check the effect of changing the gauge action on the phase structure our collaboration performed simulations with two additional gauge actions: the DBW2 gauge action [164, 165] and the tree level Symanzik (tlSym) improved gauge

[†]In the figure one can nicely see the eigenvalue free strip around the real axis, which is due to the twisted mass term serving as an infra-red cut-off to the spectrum.

action [166, 167]. Both of these belong to a one-parameter family of gauge actions and include, besides the usual (1×1) Wilson plaquette term, planar rectangular (1×2) Wilson loops:

$$\begin{aligned} S_g = \sum_x \Bigg(& c_0 \sum_{1 \le \mu < \nu; \mu,\nu=1}^{4} \frac{1}{3} \{1 - \mathrm{Re}\,\mathrm{Tr}(U_\Box)\} \\ & + c_1 \sum_{\mu \ne \nu; \mu,\nu=1}^{4} \frac{1}{3} \{1 - \mathrm{Re}\,\mathrm{Tr}(U^{1\times 2}_{x,\mu,\nu})\} \Bigg) \,, \end{aligned} \tag{4-10}$$

with the normalization condition $c_0 = 1 - 8c_1$. (The notation c_0, c_1 is conventional. c_1 should not be confused with the parameter c_1 in the effective potential model). The coefficient c_1 in Eq. (4-10) takes different values for the two choices of gauge actions mentioned above:

$$c_1 \;=\; \begin{cases} -1.4088 & \text{DBW2 gauge action} \\ -1/12 & \text{tlSym gauge action .} \end{cases} \tag{4-11}$$

Clearly, $c_1 = 0$ corresponds to the original Wilson plaquette gauge action. Note that the value of $c_1 = -0.331$ corresponds to the Iwasaki gauge action [162, 163].

The c_1 value for the DBW2 gauge action was determined by renormalization group considerations. The value of $c_1 = -1/12$ corresponds to the value computed at tree level in order to improve the gauge action à la Symanzik. Thus, the tlSym gauge action is in between the DBW2 and the Wilson plaquette gauge action, even though the numerical value of c_1 suggests that it is closer to the Wilson gauge action.

Our collaboration obtained very promising results for the DBW2 gauge action, which are published in Ref. [168]. If we tune the parameters with the DBW2 gauge action such that the lattice spacings are comparable to the one measured with Wilson plaquette gauge action at $\beta = 5.2$, we find that the strength of the phase transition is significantly reduced. Moreover, for even smaller lattice spacings, in a situation now comparable to the one with Wilson plaquette gauge action at $\beta = 5.3$, we do not find evidence for a first order phase transition. For the tlSym gauge action the investigations are still ongoing, but the preliminary results are similar to the one observed with the DBW2 gauge action. We summarize the results in figure 4.10, where we show the plaquette expectation value as a function of κ for the DBW2, the tlSym and the Wilson plaquette gauge action at approximately the same value for $a = 0.2$ fm. For all of the three actions meta-stabilities are visible. The value of $a\mu$ was only for the Wilson plaquette gauge action different from zero, which should, however, decrease the effect for the plaquette gauge action.

Passing in figure 4.10 from the Wilson over the tlSym to the DBW2 gauge action the jump in the plaquette expectation value becomes clearly smaller. In addition,

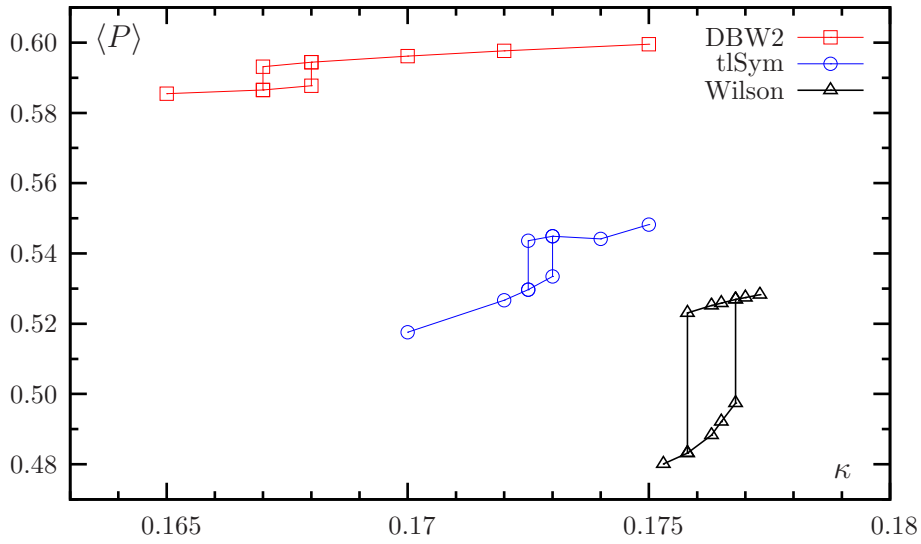

Figure 4.10: Plaquette expectation values as a function of κ for the three different gauge actions at approximately identical value of the lattice spacing $a = 0.2$ fm. For the DBW2 and the tlSym gauge action the value of μ was identical zero, whereas for the Wilson gauge action we used $a\mu = 0.013$. The continuous lines only connect the points and are meant to guide the eyes. The meta-stable region is indicated by connecting high and low phase at the first and the last meta-stable point.

the difference between DBW2 and tlSym is much smaller than the difference between tlSym and Wilson plaquette. This outcome, if confirmed, is surprising, since one could expect the effect to "scale" with c_1.

Nevertheless, these results make us confident that changing the gauge action is indeed a tool to weaken the effects of the first order phase transition, in agreement with earlier findings [150, 161]. With a different gauge action than the Wilson plaquette gauge action dynamical simulation with twisted mass fermions at maximal twist might then become possible with lattice spacings equal or lower than 0.16 fm and pseudo scalar masses small enough.

4.3 Conclusion

The main result of this chapter is that close enough to the continuum the phase structure in lattice theories with Wilson or Wilson twisted mass fermions is the expected continuum phase structure of QCD distorted by lattice artifacts.

In detail, we have explored the phase structure of lattice QCD with Wilson twisted mass fermions and the Wilson plaquette gauge action. We have investigated three values of the bare coupling $\beta = 5.1, 5.2, 5.3$ each with fixed value of $a\mu$. By changing the hopping parameter κ we encountered strong meta-stabilities for all three values of β, visible in long living meta-stable states with either a low or a high

plaquette expectation value. The PCAC quark mass m_χ^{PCAC} in the different metastable branches is positive for the branch with low plaquette expectation value and negative for the branch with high plaquette expectation value. At the same time, the pseudo scalar mass does not vanish at the chiral point but has a minimum at a rather large value, which is at $\beta = 5.3$ still about 500 MeV. We stress here that the aforementioned lower bound for the pseudo scalar mass does not originate from algorithmic or technical problems, but it is a physical property of the lattice theory. In fact, it would be interesting to investigate the phase structure of lattice QCD with different formulations, such as the staggered or even the overlap formulation.

This phenomenon finds a natural interpretation in the effective potential model from lattice chiral perturbation theory, both for pure Wilson fermions with $\mu = 0$ [41] and for Wilson twisted mass fermions with $\mu \neq 0$ [142, 97, 143]: the so-called normal scenario with a first order phase transition and a non-vanishing pseudo scalar mass at the chiral point is realized for the β value that we investigated.

We clearly observe that this first order phase transition weakens substantially, when β is increased. Unfortunately, we cannot quantitatively locate the value of the lattice spacing, where the effects of the first order phase transition becomes negligible and where a minimal pseudo scalar mass of, say, 300 MeV can be reached. As an estimate of such a value of the lattice spacing we give $a \approx 0.1\,\mathrm{fm}$. Of course, this would mean that a continuum extrapolation of physical results obtained on lattices with linear extent of at least $L = 2\,\mathrm{fm}$ would be very demanding, since the starting point for such simulations would already require large lattices. It is therefore very important to find alternative actions such that the value of the lattice spacing can be lowered without running into problems with the first order phase transition.

With our results together with results available in the literature we were able to draw a schematic picture of the phase structure of lattice QCD with Wilson like fermions. While for values of β smaller than 5.0 there is evidence for the Aoki scenario, in the range of β values between 5.1 and 5.3 we find evidence for the normal scenario. The phase diagram is summarized in fig. 4.8.

Our collaboration also investigated the change of the observed phase structure with two different gauge actions to replace the Wilson plaquette gauge action. These are the DBW2 and the tree level Symanzik improved gauge actions, both of which belong to a one-parameter family of gauge actions. The results we obtain are very promising in a sense that it seems to become possible to reduce significantly the effects of the first order phase transition at lattice spacings comparable to the one used in this chapter (see Ref. [168] for details). This makes us confident that indeed with a different gauge action than the Wilson plaquette gauge action dynamical simulations with automatic $\mathcal{O}(a)$ improved Wilson twisted mass fermions are feasible.

Finally, we remark that in the twisted mass formulation also non-degenerate

quark flavors can be simulated without loosing the property of automatic $\mathcal{O}(a)$ improvement [169, 46]. Together with the twisted mass parameter serving as an infra-red cut-off for the eigenvalue spectrum, the twisted mass formulation then becomes a promising candidate for large scale simulations with dynamical up-, down- and strange quark.